Inorg. Chem. **2005**, *44*, 8033–8043

Binuclear Wirelike Dimers Based on Ruthenium(II)–Bipyridine Units Linked by Ethynylene–Oligothiophene–Ethynylene Bridges

Andrea Barbieri,*,† Barbara Ventura,† Lucia Flamigni,† Francesco Barigelletti,† Gerda Fuhrmann,‡ Peter Bäuerle,‡ Sébastien Goeb,§ and Raymond Ziessel*,§

Istituto per la Sintesi Organica e la Fotoreattività, Consiglio Nazionale delle Ricerche (ISOF-CNR), Via P. Gobetti 101, 40129 Bologna, Italy, Department of Organic Chemistry II, University of Ulm, Albert-Einstein-Allee 11, 89081 Ulm, Germany, and Laboratoire de Chimie Moléculaire, Ecole de Chimie, Polymères, Matériaux (ECPM), Université Louis Pasteur (ULP), 25 rue Becquerel, 67087 Strasbourg Cedex 02, France

Received April 18, 2005

The syntheses, structural characteristics, electrochemical behavior, ground-state spectra, photophysical properties, and transient absorption (TA) spectra in CH_3CN solvent are reported for binuclear $[(bpy)_2Ru(bpy\text{-}E(T)_nE\text{-}bpy)Ru(bpy)_2]^{4+}$ complexes, $Ru(bpyT_nbpy)Ru$, where the Ru-based units are connected by alternating 3,4-dibutylthiophene (DBT′)/thiophene (T′) fragments linked via ethynyl groups (E) to bpy ligands at the 5-position (bpy is 2,2′-bipyridine). The ligand $bpyT_3bpy$ represents a module containing DBT′/T′/DBT′ subunits, and $bpyT_5bpy$ accounts for a DBT′/T′/DBT′/T′/DBT′ pattern. The syntheses and electrochemical and spectroscopic (emission and TA) properties in CH_2Cl_2 solvent of the $bpyT_nbpy$ ligands are likewise reported. The behavior of the $Ru(bpyT_nbpy)Ru$ dimers has been compared to that of the $bpyT_nbpy$ ligands and to that of a related mononuclear complex, $[(bpy)_2Ru(bpy\text{-}E\text{-}DBT')]^{2+}$, Ru(bpyDBT′). For the dimeric complexes, the electrochemical results show that the first reduction step takes place at the bpy ligand(s) bearing an ethynylene group, the first oxidation step is thiophene-centered, and further oxidation involves the metal centers, which are only weakly interacting. The photophysical and TA results for the $Ru(bpyT_nbpy)Ru$ dimers account for the presence of low-lying oligothiophene-centered $^3\pi,\pi^*$ levels, while higher-lying metal–ligand charge transfer (^{3}MLCT) levels are thermally accessible only for the case of $Ru(bpyT_3\text{-}bpy)Ru$; the possible role of charge separation (CS) levels (from oxidation at the thiophene bridge and reduction at one of the coordinated bpy's) is also discussed.

Introduction

Hybrid conjugated materials that contain oligothiophene wires are opening interesting perspectives for the development of technologies for electronics and optoelectronics.[1−8] The combination of ruthenium(II)−polypyridine complexes and thiophene-based oligomers offers a series of advantages and is being actively pursued.[9−20] These advantages include the fact that mononuclear and polynuclear ruthenium(II)−polypyridine compounds have been one of the most studied families of compounds over the past decades, given the impressive collection of optical absorption, emission, and

* To whom correspondence should be addressed. E-mail: andrea.barbieri@isof.cnr.it (A.B.), ziessel@chimie.u-strasbg.fr (R.Z.).
† Consiglio Nazionale delle Ricerche.
‡ University of Ulm.
§ Université Louis Pasteur.

(1) Swager, T. M. *Acc. Chem. Res.* **1998**, *31*, 201.
(2) Bäuerle, P. In *Electronic Materials: The Oligomeric Approach*; Müllen, K., Wegner, G., Eds.; Wiley-VCH: Weinheim, Germany, 1998; Chapter 2.
(3) Roncali, J. *J. Mater. Chem.* **1999**, *9*, 1875.
(4) Mitschke, U.; Bäuerle, P. *J. Mater. Chem.* **2000**, *10*, 1471.
(5) Roncali, J. *Acc. Chem. Res.* **2000**, *33*, 147.
(6) Tour, J. M. *Acc. Chem. Res.* **2000**, *33*, 791.
(7) Otsubo, T.; Aso, Y.; Takimiya, K. *J. Mater. Chem.* **2002**, *12*, 2565.
(8) Cravino, A.; Zerza, G.; Neugebauer, H.; Maggini, M.; Bucella, S.; Menna, E.; Svensson, M.; Andersson, M. R.; Brabec, C. J.; Sariciftci, N. S. *J. Phys. Chem. B* **2002**, *106*, 70.
(9) Zhu, S. S.; Kingsborough, R. P.; Swager, T. M. *J. Mater. Chem.* **1999**, *9*, 2123.
(10) Constable, E. C.; Housecroft, C. E.; Schofield, E. R.; Encinas, S.; Armaroli, N.; Barigelletti, F.; Flamigni, L.; Figgemeier, E.; Vos, J. G. *Chem. Commun.* **1999**, 869.
(11) Walters, K. A.; Trouillet, L.; Guillerez, S.; Schanze, K. S. *Inorg. Chem.* **2000**, *39*, 5496.
(12) Pappenfus, T. M.; Mann, K. R. *Inorg. Chem.* **2001**, *40*, 6301.
(13) Encinas, S.; Flamigni, L.; Barigelletti, F.; Constable, E. C.; Housecroft, C. E.; Schofield, E. R.; Figgemeier, E.; Fenske, D.; Neuburger, M.; Vos, J. G.; Zehnder, M. *Chem.—Eur. J.* **2002**, *8*, 137.
(14) Liu, Y.; De Nicola, A.; Reiff, O.; Ziessel, R.; Schanze, F. S. *J. Phys. Chem. A* **2003**, *107*, 3476.

10.1021/ic050596x CCC: $30.25
Published on Web 09/23/2005

electrochemical properties exhibited by these complexes;[21−30] actually, on the basis of these properties, this family of complexes proves of use for optoelectronic applications.[31−35] On the other hand, poly- and oligothiophenes are most attractive compounds in themselves, particularly promising for the development of molecular wires, and their optical and electrochemical properties are likewise extensively studied, particularly for the smaller oligomers.[2,4,36−47] Furthermore, they have been used as electron donors in an extended series of donor−acceptor systems able to undergo photoinduced charge separation.[8,48−53]

Inclusion of ruthenium(II)−polypyridine complexes, and other metal centers,[15] as side or end units of linearly arranged oligothiophene frameworks may result in a unique combination of photophysical and electrochemical properties. This is particularly appealing bearing in mind that the oligothiophene backbone can behave as a conducting entity for electron and excitation energy transfer.[9,54] Therefore, for these hybrid materials, it is of importance to investigate and understand the nature and energetic and spatial location of the various excited states, with particular emphasis on the lowest-lying ones, originated by the integration of ruthenium(II)−polypyridine and oligothiophene units.

Here, we present the preparation of two such molecular wires, $[(bpy)_2Ru(bpy\text{-}E(T)_nE\text{-}bpy)Ru(bpy)_2]^{4+}$, $Ru(bpyT_3\text{-}bpy)Ru$ and $Ru(bpyT_5bpy)Ru$ for $n = 3$ and 5, respectively. Here, the terminal $[Ru(bpy)_3]^{2+}$ units are connected via an alternation of 3,4-dibutylthiophene (DBT′) and thiophene (T′) fragments linked by ethynyl bonds (E) at the 5-position of coordinated bpy ligands (bpy is 2,2′-bipyridine) (see Chart 1). The estimated metal-to-metal distance is 24.1 and 31.4 Å for $Ru(bpyT_3bpy)Ru$ and $Ru(bpyT_5bpy)Ru$, respectively (from ZINDO/1 semiempirical self-consistent field (SCF) calculations according to Hyperchem 7.5). The electrochemical and optical characterization of these complexes is expected to provide insights into the establishment of excitonic type delocalization within thiophene-based oligomers, an electronic effect known to be length-dependent.[41,46,47,55] In particular, our study is aimed at understanding (i) the role of the various excited states, including those that originated from possible charge separation (CS) processes,[49,51] that in our cases may be present at the interface between the terminals and the oligothiophene bridge, and (ii) the electronic layout that exists within this type of molecular wire.

Experimental Section

General Methods. The 400.1 (^{1}H) and 100.6 MHz (^{13}C) NMR spectra were recorded at room temperature using residual proton or carbon signals, respectively, of the deuterated solvents as internal references. FT-IR spectra were recorded on the compounds as neat liquids or thin films, prepared with a drop of CH_2Cl_2 and evaporated to dryness on KBr pellets. Chromatographic purification was conducted using 40−63 μm silica gel or aluminum oxide 90 standardized. Thin-layer chromatography (TLC) was performed on silica gel or aluminum oxide plates coated with fluorescent indicator. Deactivated plates were previously treated with 90:10 CH_2Cl_2−Et_3N. All mixtures of solvents are given in v/v ratios. The experimental procedures for each reaction were tested several times to optimize conditions.

(15) Liu, Y.; Li, Y.; Schanze, K. S. *J. Photochem. Photobiol., C* **2002**, 1.
(16) Cunningham, G. B.; Li, Y. T.; Liu, S. X.; Schanze, K. S. *J. Phys. Chem. B* **2003**, *107*, 12569.
(17) Barbieri, A.; Ventura, B.; Barigelletti, F.; De Nicola, A.; Quesada, M.; Ziessel, R. *Inorg. Chem.* **2004**, *43*, 7359.
(18) Benniston, A. C.; Harriman, A.; Lawrie, D. J.; Mayeux, A. *Phys. Chem. Chem. Phys.* **2004**, *6*, 51.
(19) Hjelm, J.; Handel, R. W.; Hagfeldt, A.; Constable, E. C.; Housecroft, C. E.; Forster, R. J. *Inorg. Chem.* **2005**, *44*, 1073.
(20) Houarner, C.; Blart, E.; Buvat, P.; Odobel, F. *Photochem. Photobiol. Sci.* **2005**, *4*, 200.
(21) Kalyanasundaram, K. *Coord. Chem. Rev.* **1982**, *46*, 159.
(22) Juris, A.; Balzani, V.; Barigelletti, F.; Campagna, S.; Belser, P.; von Zelewsky, A. *Coord. Chem. Rev.* **1988**, *84*, 85.
(23) Meyer, T. J. *Pure Appl. Chem.* **1986**, *58*, 1193.
(24) Balzani, V.; Juris, A.; Venturi, M.; Campagna, S.; Serroni, S. *Chem. Rev.* **1996**, *96*, 759.
(25) Harriman, A.; Ziessel, R. *Chem. Commun.* **1996**, 1707.
(26) De Cola, L.; Belser, P. *Coord. Chem. Rev.* **1998**, *177*, 301.
(27) Barigelletti, F.; Flamigni, L. *Chem. Soc. Rev.* **2000**, *29*, 1.
(28) Anderson, P. A.; Keene, F. R.; Meyer, T. J.; Moss, J. A.; Strouse, G. F.; Treadway, J. A. *J. Chem. Soc., Dalton Trans.* **2002**, 3820.
(29) Tor, Y. *C. R. Chim.* **2003**, *6*, 755.
(30) Huynh, M. H. V.; Dattelbaum, D. M.; Meyer, T. J. *Coord. Chem. Rev.* **2005**, *249*, 457.
(31) Adams, D. M.; Brus, L.; Chidsey, C. E. D.; Creager, S.; Creutz, C.; Kagan, C. R.; Kamat, P. V.; Lieberman, M.; Lindsay, S.; Marcus, R. A.; Metzger, R. M.; Michel-Beyerle, M. E.; Miller, J. R.; Newton, M. D.; Rolison, D. R.; Sankey, O.; Schanze, K. S.; Yardley, J.; Zhu, X. Y. *J. Phys. Chem. B* **2003**, *107*, 6668.
(32) Stott, T. L.; Wolf, M. O. *Coord. Chem. Rev.* **2003**, *246*, 89.
(33) Scandola, F. In *Encyclopedia of Supramolecular Chemistry*; Atwood, J. L., Steed, J. W., Eds.; Marcel Dekker: New York, 2004; p 535.
(34) Coe, B. J.; Curati, N. R. M. *Comments Inorg. Chem.* **2004**, *25*, 147.
(35) Holliday, B. J.; Swager, T. M. *Chem. Commun.* **2005**, 23.
(36) Belletete, M.; Mazerolle, L.; Desrosiers, N.; Leclerc, M.; Durocher, G. *Macromolecules* **1995**, *28*, 8587.
(37) Chan, H. S. O.; Ng, S. C. *Prog. Polym. Sci.* **1998**, *23*, 1167.
(38) Kraft, A.; Grimsdale, A. C.; Holmes, A. B. *Angew. Chem., Int. Ed.* **1998**, *37*, 402.
(39) Martin, R. E.; Diederich, F. *Angew. Chem., Int. Ed.* **1999**, *38*, 1350.
(40) Noda, T.; Ogawa, H.; Noma, N.; Shirota, Y. *J. Mater. Chem.* **1999**, *9*, 2177.
(41) Apperloo, J. J.; Janssen, R. A. J.; Malenfant, P. R. L.; Frechet, J. M. J. *J. Am. Chem. Soc.* **2001**, *123*, 6916.
(42) Rothe, C.; Hintschich, S.; Monkman, A. P.; Svensson, M.; Anderson, M. R. *J. Chem. Phys.* **2002**, *116*, 10503.
(43) Barbarella, G. *Chem.−Eur. J.* **2002**, *8*, 5072.
(44) De Nicola, A.; Liu, Y.; Schanze, K. S.; Ziessel, R. *Chem. Commun.* **2003**, 288.
(45) De Nicola, A.; Ringenbach, C.; Ziessel, R. *Tetrahedron Lett.* **2003**, *44*, 183.
(46) Izumi, T.; Kobashi, S.; Takimiya, K.; Aso, Y.; Otsubo, T. *J. Am. Chem. Soc.* **2003**, *125*, 5286.
(47) Ringenbach, C.; De Nicola, A.; Ziessel, R. *J. Org. Chem.* **2003**, *68*, 4708.
(48) Matsumoto, K.; Fujitsuka, M.; Sato, T.; Onodera, S.; Ito, O. *J. Phys. Chem. B* **2000**, *104*, 11632.
(49) van Hal, P. A.; Knol, J.; Langeveld-Voss, B. M. W.; Meskers, S. C. J.; Hummelen, J. C.; Janssen, R. A. J. *J. Phys. Chem. A* **2000**, *104*, 5974.
(50) van Hal, P. A.; Beckers, E. H. A.; Meskers, S. C. J.; Janssen, R. A. J.; Jousselme, B.; Blanchard, P.; Roncali, J. *Chem.−Eur. J.* **2002**, *8*, 5415.
(51) Araki, Y.; Luo, H. X.; Nakamura, T.; Fujitsuka, M.; Ito, O.; Kanato, H.; Aso, Y.; Otsubo, T. *J. Phys. Chem. A* **2004**, *108*, 10649.
(52) Kanato, H.; Takimiya, K.; Otsubo, T.; Aso, Y.; Nakamura, T.; Araki, Y.; Ito, O. *J. Org. Chem.* **2004**, *69*, 7183.
(53) Fron, E.; Lor, M.; Pilot, R.; Schweitzer, G.; Dincalp, H.; De Feyter, S.; Cremer, J.; Bäuerle, P.; Müllen, K.; Van der Auweraer, M.; De Schryver, F. C. *Photochem. Photobiol. Sci.* **2005**, *4*, 61.
(54) Ziessel, R.; Bäuerle, P.; Ammann, M.; Barbieri, A.; Barigelletti, F. *Chem. Commun.* **2005**, 802.
(55) Odobel, F.; Suresh, S.; Blart, E.; Nicolas, Y.; Quintard, J. P.; Janvier, P.; Le Questel, J. Y.; Illien, B.; Rondeau, D.; Richomme, P.; Haupl, T.; Wallin, S.; Hammarström, L. *Chem.−Eur. J.* **2002**, *8*, 3027.

Chart 1

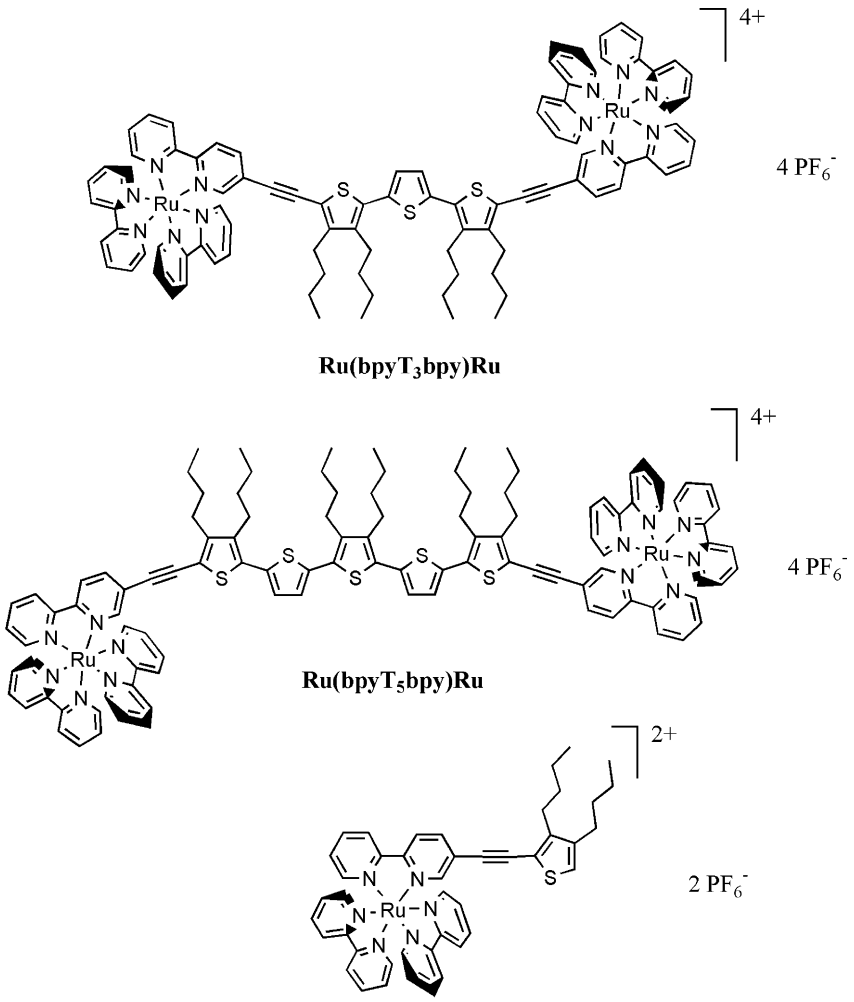

5,5″-Diiodo-3,3″,4,4″-tetrabutyl-2,2′:5′,2″-terthiophene (T_3I_2). To a solution of 3,3″,4,4″-tetrabutyl-2,2′:5′,2″-terthiophene[56] (10.0 g, 20.9 mmol) in CH_2Cl_2 (200 mL) was added mercuric acetate (14.7 g, 46.0 mmol) and acetic acid (2.76 g, 46.0 mmol). The reaction mixture was stirred at ambient temperature for 8 h. After addition of iodine (11.7 g, 46.0 mmol) at 0 °C, it was allowed to warm to room temperature and stirred for 3 h. The reaction mixture was quenched with saturated NaS_2O_3 solution and extracted with CH_2Cl_2. The organic layer was washed with saturated $NaHCO_3$ solution and water and was dried over Na_2SO_4. After evaporation of the solvent, the crude product was purified by column chromatography on silica gel (petrol ether). Yield: 91% **T_3I_2** (13.8 g, 19.0 mmol) as a yellow solid. Mp: 57/8 °C. HPLC (*n*-hexane/CH_2Cl_2 98:2): t_R (λ_{max}) 4.8 min (347 nm). ^{1}H NMR ($CDCl_3$): δ 6.98 (s, 2H, H-3′,4′-*Th*), 2.74 (t, $^3J_{(\alpha',\beta'-CH_2-Bu),(\alpha'',\beta''-CH_2-Bu)}$ = 7.8 Hz, 4H, α′,α″-CH_2-*Bu*), 2.53 (t, $^3J_{(\alpha,\beta-CH_2-Bu),\ (\alpha''',\beta'''-CH_2-Bu)}$ = 7.6 Hz, 4H, α,α‴-CH_2-*Bu*), 1.48 (m, 16H, $\beta-\beta'''$,γ- γ'''-CH_2-*Bu*), 0.98 (m, 12H, CH_3-*Bu*). ^{13}C NMR ($CDCl_3$): δ 147.5 (C-2′,5′-*Th*), 138.7 (C-4,4″-*Th*), 135.8 (C-2,2″,3,3″-*Th*), 126.2 (C-3′,4′-*Th*), 74.2 (C-5,5″-*Th*), 33.0, 32.1 ($\beta-\beta'''$-CH_2-*Bu*), 31.0, 28.3 (α−α‴-CH_2-*Bu*), 22.9 ($\gamma-\gamma'''$-CH_2-*Bu*), 13.9, 13.8 (CH_3-*Bu*). MS (EI, 70 eV): *m*/z (%) 726 (18) [M^+], 725 (39) [M^+], 724 (100) [M^+]. Anal. Calcd for $C_{28}H_{38}I_2S_3$ (M_w = 724.62): C, 46.41; H, 5.29; S, 13.27. Found: C, 46.36; H, 5.33; S, 13.43.

General Procedure for the Preparation of the Ligands. A Schlenk flask was charged with a benzene solution (20 mL) containing 1 equiv of T_3I_2 (100 mg scale) or $T_5(TMS)_2$[56] (100 mg scale) and 2 equiv of 5-ethynyl-2,2′-bipyridine[57] or 5-bromo-2,2′-bipyridine[58] derivatives, respectively. An aqueous solution (20 mL) containing benzyltriethylammonium chloride ([$BzEt_3N$]Cl, 1 mol %) and 10 equiv of NaOH was argon degassed and added to the previous organic solution. After vigorous degassing with argon, CuI (10 mol %) and [$Pd(PPh_3)_4$] (6 mol %) were finally added. The resulting yellow solution was heated at 60 °C until complete consumption of the starting material occurred (determined by TLC, the usual reaction time was 8−12 h), and then, the solvent was evaporated under vacuum. The residue was treated with water and extracted with CH_2Cl_2. The organic extracts were washed with water and then with brine and were dried over magnesium sulfate. The solvent was removed by rotary evaporation. The residue was purified by chromatography on alumina using, as eluent, a mixture of CH_2Cl_2 and cyclohexane with a gradient of cyclohexane from

(56) Krömer, J.; Bäuerle, P. *Tetrahedron* **2001**, *57*, 3785.

(57) Grosshenny, V.; Romero, F. M.; Ziessel, R. *J. Org. Chem.* **1997**, *62*, 1491.

(58) Romero, F. M.; Ziessel, R. *Tetrahedron Lett.* **1995**, *36*, 6471.

50 to 10% (v/v), followed by recrystallization in a mixture of dichloromethane/methanol/hexane.

(A) bpyT$_3$bpy. Isolated yield: 86%. Mp: 104−106 °C. ^{1}H NMR ($CDCl_3$): δ 8.78 (s, 2H), 8.69 (d, ^3J = 4.7 Hz, 2H), 8.42 (d, ^3J = 8.3 Hz, 4H), 7.89 (dd, ^3J = 8.3 Hz, ^4J = 2.1 Hz, 2H), 7.83 (td, ^3J = 7.7 Hz, ^4J = 2.0 Hz, 2H), 7.32 (td, ^3J = 4.7 Hz, ^4J = 2.0 Hz, 2H), 7.13 (s, 2H), 2.76 (m, 8H), 1.67 (m, 8H), 1.48 (m, 8H), 1.01 (m, 12H). ^{13}C{^{1}H} normal and DEPT (100.6 MHz, $CDCl_3$): δ 155.9 (C_q), 155.1 (C_q), 151.6, 149.8, 139.2, 137.3, 136.5 (C_q), 133.0 (C_q), 126.9, 124.3, 121.7, 120.8, 117.1 (C_q), 93.8 (C_q), 87.5 (C_q), 33.2 (CH_2), 29.0 (CH_2), 28.3 (CH_2), 23.4 (CH_2), 23.2 (CH_2), 14.4 (CH_3), 14.3 (CH_3). UV−vis (CH_3CN): λ [nm] (ϵ [M^{-1} cm^{-1}]) 399 (56 700), 296 (36 300). FT-IR (KBr): 2951.9, 2925.1, 2855.6, 2192.5 ($\nu_{C\equiv C}$), 1586.7, 1570.7, 1541.3, 1458.7, 1432.0, 794.7, 744.0. FAB$^+$ *m*/*z* (nature of the peak, relative intensity): 829.1 ([M + H]$^+$, 100). Anal. Calcd for $C_{52}H_{52}N_4S_3$ (M_w = 829.19): C, 75.32; H, 6.32; N 6.76. Found: C, 75.22; H, 6.08; N, 6.49.

(B) bpyT$_5$bpy. Isolated yield: 42%. Mp: 130−132 °C. ^{1}H NMR ($CDCl_3$): δ 8.80 (s, 2H), 8.69 (d, ^4J = 3.7 Hz, 2H), 8.43 (d, ^3J = 8.0 Hz, 4H), 7.90 (dd, ^3J = 8.2 Hz, ^4J = 2.0 Hz, 2H), 7.84 (td, ^3J = 7.7 Hz, ^4J = 2.0 Hz, 2H), 7.33 (td, ^3J = 3.7 Hz, ^4J = 2.0 Hz, 2H), 7.13 (s, 4H), 2.77 (m, 12H), 1.59 (m, 12H), 1.49 (m, 12H), 1.00 (m, 18H). ^{13}C{^{1}H} normal and DEPT ($CDCl_3$): δ 155.9 (C_q), 155.0 (C_q), 151.6, 149.9, 149.7, 140.8 (C_q), 139.2, 139.1, 137.3, 136.9 (C_q), 136.0 (C_q), 133.2 (C_q), 130.2 (C_q), 126.9, 126.5, 124.3, 121.7, 120.9, 120.8, 117.0 (C_q), 93.8 (C_q), 87.6 (C_q), 33.3 (CH_2), 33.2 (CH_2), 30.1 (CH_2), 29.0 (CH_2), 28.4 (CH_2), 28.3 (CH_2), 23.5 (CH_2), 23.4 (CH_2), 23.3 (CH_2), 14.4 (CH_3), 14.3 (CH_3). UV−vis (CH_3CN): λ [nm] (ϵ [M^{-1} cm^{-1}]) 410 (70 000), 288 (37 600). FT-IR (KBr): 2951.9, 2930.5, 2855.6, 2192.5 ($\nu_{C\equiv C}$), 1586.7, 1570.7, 1541.3, 1456.0, 1432.0, 794.7, 744.0. FAB$^+$ *m*/*z* (nature of the peak, relative intensity): 1105.1 ([M + H]$^+$, 100). Anal. Calcd for $C_{68}H_{72}N_4S_5$ (M_w = 1105.65): C, 73.87; H, 6.56; N, 5.07. Found: C, 73.79; H, 6.29; N, 4.71.

General Procedure for the Preparation of the Ruthenium Complexes. In a Schlenk flask, a stirred CH_2Cl_2 solution containing 1 equiv of the ligand was treated with an ethanol solution containing 2 equiv of $[Ru(bpy)_2]Cl_2 \cdot 2H_2O$[59] and heated at 60 °C overnight. After complete consumption of starting material occurred (determined by TLC), an aqueous solution (5 equiv) of KPF_6 was added; the organic solvent was then removed under vacuum, and the precipitates were washed by centrifugation with water until the solution was colorless. The target complexes were purified by chromatography on alumina eluting with CH_2Cl_2 using a gradient of methanol. The pure red complexes were obtained by double recrystallization in acetone/hexane.

(A) Ru(bpyT$_3$bpy)Ru. Isolated yield: 76%. ^{1}H NMR (d_6-acetone): δ 8.82 (5 lines multiplet, 12H), 8.22 (9 lines multiplet, 14H), 8.06 (6 lines multiplet, 10H), 7.59 (9 lines multiplet, 10H), 7.29 (s, 2H), 2.79 (m, overlapping with residual water), 2.68 (m, 4H), 1.54 (7 lines multiplet, 8H), 1.45 (6 lines multiplet, 4H), 1.35 (6 lines multiplet, 4H), 0.94 (t, ^3J = 7.5 Hz, 6H), 0.92 (t, ^3J = 7.5 Hz, 6H). ^{13}C{^{1}H} normal and DEPT (100.6 MHz, d_6-acetone): δ 158.0 (C_q), 157.9 (C_q), 157.9 (C_q), 157.9 (C_q), 157.4 (C_q), 156.8 (C_q), 153.3, 152.9, 152.7, 152.6, 152.4, 151.8 (C_q), 140.1, 139.8, 138.9, 138.9, 138.8, 128.7, 128.7, 128.58, 128.56, 128.2, 125.6, 125.3, 125.2, 124.8, 124.4, 116.1 (C_q), 92.4 (C_q), 90.4 (C_q), 33.1 (CH_2), 33.0 (CH_2), 30.1 (CH_2), 23.3 (CH_2), 23.1 (CH_2), 14.1 (CH_3), 13.9 (CH_3). UV−vis (CH_3CN): λ [nm] (ϵ [M^{-1} cm^{-1}]) 442 (77 500), 288 (146 800). FT-IR (KBr): 2954.2, 2927.2, 2867.9, 2188.7 ($\nu_{C\equiv C}$), 1602.2, 1591.4, 1465.0, 1446.2, 838.7 (ν_{PF}), 766.1, 728.5, 556.5. ES-MS in CH_3CN (nature of the peak, relative intensity): 2091.2 ([M − PF_6]$^+$, 100); 973.2 ([M − 2PF_6]$^{2+}$, 45); 600.1 ([M − 3PF_6]$^{3+}$, 20). Anal. Calcd for $C_{92}H_{84}N_{12}S_3Ru_2P_4F_{24}$ (M_w = 2235.92): C, 49.42; H, 3.79; N, 7.52. Found: C, 49.19; H, 3.83; N, 7.65.

(B) Ru(bpyT$_5$bpy)Ru. Isolated yield: 63%. ^{1}H NMR (d_6-acetone): δ 8.83 (10 lines multiplet, 12H), 8.21 (14 lines multiplet, 14H), 8.06 (7 lines multiplet, 10H), 7.60 (14 lines multiplet, 10H), 7.28 (AB quartet, ^3J = 8.0 Hz, 4H), 2.80 (m, overlapping with residual water), 2.69 (m, 4H), 1.64−1.33 (m, 24H), 0.95 (9 lines multiplet, 18H). ^{13}C{^{1}H} (d_6-acetone): δ 158.3, 158.2, 158.1, 158.1, 157.6, 156.9, 153.5, 153.1, 152.9, 152.8, 152.6, 152.0, 141.7, 140.07, 140.02, 139.1, 139.1, 139.0, 137.4, 135.8, 134.8, 130.5, 128.89, 128.86, 128.8, 128.7, 128.3, 127.6, 125.8, 125.5, 125.4, 125.0, 124.7, 116.1 (C_q), 92.5 (C_q), 90.8 (C_q), 33.6 (CH_2), 33.4 (CH_2), 33.3 (CH_2), 23.6 (CH_2), 23.5 (CH_2), 23.3 (CH_2), 14.13 (CH_3), 14.10 (CH_3). UV−vis (CH_3CN): λ [nm] (ϵ [M^{-1} cm^{-1}]) 445 (100 700), 287 (187 200). FT-IR (KBr): 2954.2, 2927.2, 2867.9, 2188.7 ($\nu_{C\equiv C}$), 1602.1, 1591.4, 1462.4, 1446.2, 836.0 (ν_{PF}), 760.7, 731.2, 556.5. ES-MS in CH_3CN (nature of the peak, relative intensity) 2367.1 ([M − PF_6]$^+$, 100); 1111.2 ([M − 2PF_6]$^{2+}$, 35); 692.5 ([M − 3PF_6]$^{3+}$, <10). Anal. Calcd for $C_{108}H_{104}N_{12}S_5Ru_2P_4F_{24}$ (M_w = 2512.38): C, 51.63; H, 4.17; N, 6.69. Found: C, 51.84; H, 4.32; N, 6.50.

Electrochemical Measurements. Electrochemical studies employed cyclic voltammetry with a conventional three-electrode system using a BAS CV-50W voltammetric analyzer equipped with a Pt microdisk (2 mm^2) working electrode and a platinum wire counter electrode. Ferrocene was used as an internal standard and was calibrated against a saturated calomel reference electrode (SCE, Fc^+/Fc = 0.39 V) separated from the electrolysis cell by a glass frit presoaked with electrolyte solution. Solutions contained the electroactive substrate (ca. 5.0 × 10^{-3} M) in deoxygenated and anhydrous CH_3CN with tetra-*n*-butylammonium hexafluorophosphate (0.1 M) as the supporting electrolyte. The quoted half-wave potentials were reproducible within ±10 mV.

Optical Spectroscopy. Absorption spectra of dilute solutions (2 × 10^{-5} M) of CH_2Cl_2 (for the ligands) and CH_3CN (for the complexes) were obtained with a Perkin-Elmer Lambda 45 UV−vis spectrometer. For luminescence experiments, the samples were placed in fluorimetric 1 cm path cuvettes and, when necessary, purged from oxygen by bubbling with argon or by evacuating with repeated freeze−pump−thaw cycles. Uncorrected luminescence spectra were obtained either with a Spex Fluorolog II spectrofluorimeter, equipped with a Hamamatsu R928 phototube, or with an Edinburgh FLS920 spectrometer (continuous 450 W Xe lamp), equipped with a peltier-cooled Hamamatsu R928 photomultiplier tube (185−850 nm). Sample solutions were excited at the indicated wavelength, and dilution was adjusted to obtain absorbance values ≤ 0.15. While uncorrected luminescence band maxima are used throughout the text, corrected spectra were employed for the determination of the luminescence quantum yields. The correction procedure is based on use of software, which takes care of the wavelength-dependent phototube response. From the wavelength-integrated area of the corrected luminescence spectra, we obtained luminescence quantum yields ϕ_{em} for the samples with reference to $[Ru(bpy)_3]Cl_2$ (ϕ_r = 0.028 in air-equilibrated water[60]) and by using eq 1,[61]

$$\frac{\phi_{em}}{\phi_r} = \frac{(Abs)_r \eta^2 (area)}{(Abs)\eta_r^2 (area)_r} \quad (1)$$

(59) Sullivan, B. P.; Salmon, D. J.; Meyer, T. J. *Inorg. Chem.* **1978**, *17*, 3334.

where Abs and η are absorbance values and the refractive index of the solvent, respectively. Band maxima and relative luminescence intensities were affected by an uncertainty of 2 nm and 20%, respectively. Luminescence lifetimes longer than 1 ns were obtained using an IBH 5000F single-photon counting spectrometer. Excitation was performed by using 375 and 465 nm nanoled sources. Analysis of the luminescence decay profiles against time was accomplished using software provided by the manufacturers. Within an overall resolution of 20 ps, the lifetime values were obtained with an estimated uncertainty of 10%. Luminescence lifetimes shorter than 1 ns were determined by an apparatus based on an Nd:YAG laser (Continuum PY62-10) with a 35 ps pulse duration (355 nm, 1 mJ per pulse) and a Streak camera (Hamamatsu C1587 equipped with a M1952). The luminescence signals from 100 laser shots were averaged, and the time profile was measured from the streak image in a wavelength range of ca. 10 nm around the maximum emission wavelength. The fittings of the luminescence decays were performed by standard iterative nonlinear programs taking into consideration the instrumental response.

Transient absorbance measurements in the nano- and microsecond range made use of a laser flash photolysis apparatus based on an Nd:YAG laser (JK Lasers) delivering pulses of 18 ns at 355 nm. The absorbance of the solutions at the exciting wavelength was ca. 1, and the energy used was 0.5 mJ per pulse (5 mJ cm^{-2}). The experimental setup used a right angle geometry between excitation and analysis, and only the first millimeter of irradiated solution was analyzed. Experiments were conducted in homemade, 10 mm × 10 mm optical cells, bubbled with argon for 20 min, if not otherwise specified. Depending on the time scale explored, either microseconds or nanoseconds, two different configurations were used. The "fast" configuration with nanosecond resolution made use of a pulsed Xenon lamp as the analyzing light and a photomultiplier with a dynode chain voltage supply modified to have a nanosecond response. The "slow" configuration made use of a Xenon steady light as the analyzing light and a photomultiplier with a dynode chain supply modified to have the maximum gain. The signals acquired by a digital scope were processed with homemade programs. To determine the reaction rate with oxygen, the decay of the transients in air-equilibrated solutions was determined and the oxygen concentration was taken to be 1.9×10^{-3} and 2.2×10^{-3} M in CH_3CN and CH_2Cl_2, respectively.[62] The estimated errors were 10% for lifetimes and 20% for quantum yields, and the working temperature, if not otherwise specified, was 295 ± 2 K.

Results and Discussion

As anticipated from our previous studies,[44] the classical route to produce ethynyl linked multitopic ligands is not effective in this case.[58] Indeed, we observe that cross-coupling of T_3I_2 with 5-ethynyl-2,2′-bipyridine (**1**)[58] or the bis-terminal alkyne (**2**)[58] with 5-bromo-2,2′-bipyridine[59] in the presence of Pd(0) promoters failed to produce the target ligands. In our hands, intractable mixtures of compounds are produced, resulting from the weak chemical stability of the terminal alkynes and the low reactivity of the halogenated derivatives. As a suitable synthetic route, we choose to start with the trimethylsilyl-protected building blocks in a one-pot reaction including a mixture of nonmiscible solvents and all the ingredients needed to promote deprotection of the alkyne and cross-coupling with the halogenated substrates.[63] The synthetic pathway to bpyT_3bpy and bpyT_5bpy is sketched in Scheme 1.

The key step in the preparation is the in-situ deprotection of the alkynes. The hydroxide anion is transported from the aqueous phase to the organic phase via benzyltriethylammonium chloride ([$BzEt_3N$]Cl, phase transfer catalyst). The nascent terminal alkyne then reacts with T_3I_2 or 5-bromo-2,2′-bipyridine to provide, respectively, the target ligands bpyT_3bpy and bpyT_5bpy. All contaminants inherent to such a phase transfer reaction are eliminated by water extraction and careful column chromatography. Double recrystallization in adequate solvents affords the pure ligands, which were characterized by NMR, microanalysis, FT-IR, mass spectrometry, UV−vis, and photoluminescence.

The empty coordination sites were saturated by refluxing the ligands with stoichiometric amounts of [$Ru(bpy)_2$]Cl_2·$2H_2O$[59] in a mixture of dichloromethane/ethanol. Exchange of the anion to hexafluorophosphate allows purification by column chromatography. The schematic structures of the complexes that are the focus of the present investigation are illustrated in Chart 1.

The fingerprint of the proton NMR spectra of the ligands is the six well-distinguished patterns corresponding to the nonsymmetric bipyridine and to the thiophene protons which resonate at 7.13 ppm (Figure S1a for bpyT_3bpy). Integration of the aromatic and methylene protons of the thiophene subunit allows for the conclusion that the double cross-linking of two ethynyl bipyridine modules has been realized in both ligands. In the ^{13}C spectrum, both sp-carbons are well resolved as singlets at 93.8 and 87.5 ppm for the two ligands. The latter signals correspond to the sp-carbon attached to the bipyridine side.

It is worth noting that, by complexation of the ditopic ligand with bulky dicationic ruthenium bis-bipyridine units, the NMR spectrum is significantly perturbed (Figure S1c for Ru(bpyT_3bpy)Ru). In particular, the well-defined triplet, likely corresponding to the 4′-protons of the bipyridine units, is shifted upfield by 0.2 ppm, while the other patterns are also shifted accordingly but overlap with the one corresponding to the protons of the unsubstituted bipyridine ligands.

A similar charge effect is found for the sp-carbon directly linked to the bipyridine, which is significantly shifted upfield by ca. 3 ppm (at 92.4 and 90.8 ppm, respectively, for Ru(bpyT_3bpy)Ru and Ru(bpyT_5bpy)Ru). Accordingly, the C≡C stretching vibrations are nicely resolved and shifted from 2192 cm^{-1} in the free ligands to 2188 cm^{-1} in the binuclear complexes. For both tetracationic complexes, electrospray mass spectroscopy (MS) exhibits well-resolved peaks corresponding to the mono-, di-, and tricationic species with the expected isotropomeric patterns.

Electrochemistry. The electrochemical properties of the two ligands in CH_2Cl_2 and the two complexes in CH_3CN

(60) Nakamaru, K. *Bull. Chem. Soc. Jpn.* **1982**, *55*, 2967.
(61) Demas, J. N.; Crosby, G. A. *J. Phys. Chem.* **1971**, *75*, 991.
(62) Murov, S. L.; Carmichael, I.; Hug, G. L. *Handbook of Photochemistry*; M. Dekker: New York, 1993.
(63) Carpita, A.; Lessi, A.; Rossi, R. *Synthesis* **1984**, 571.

Scheme 1[a]

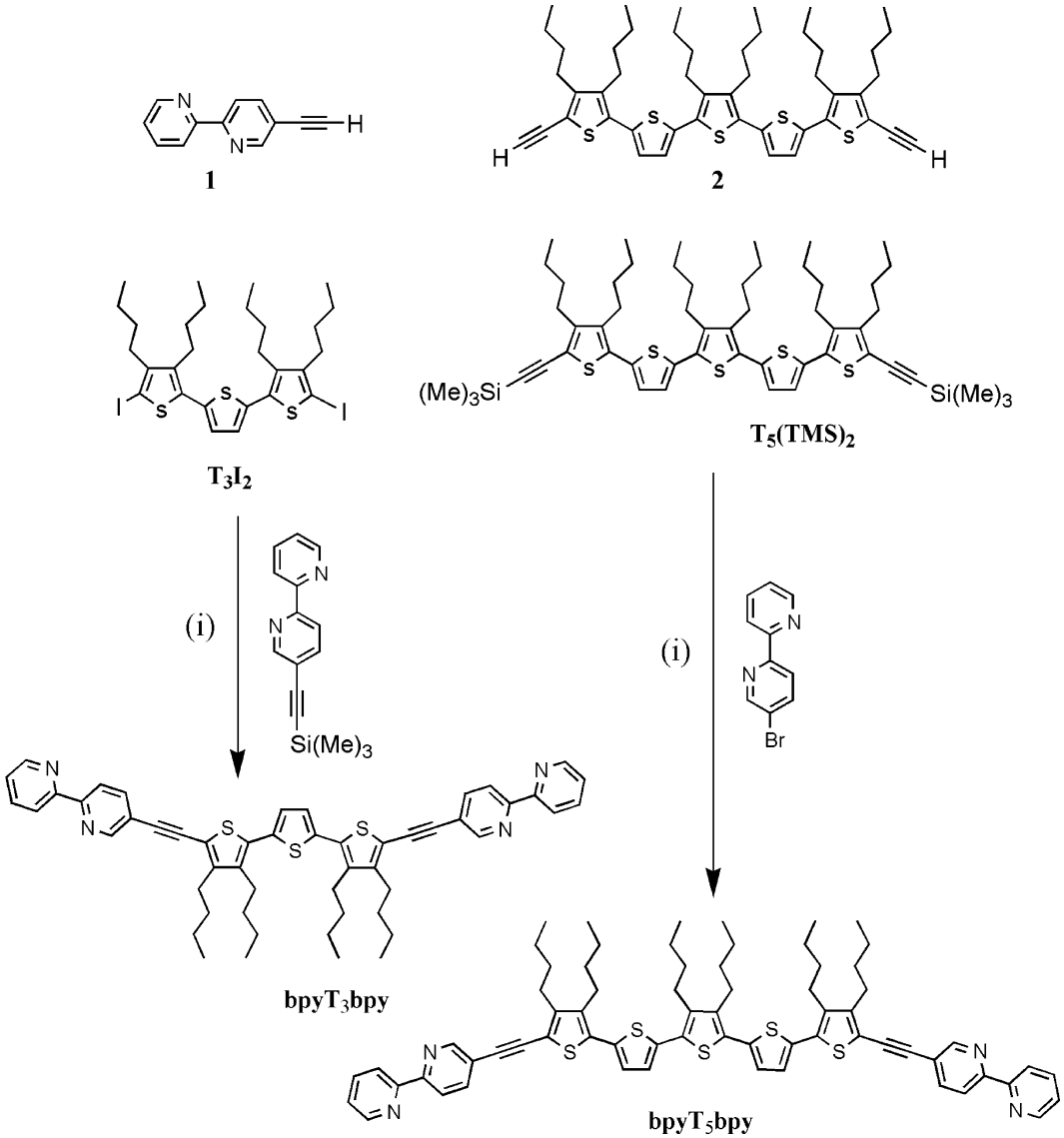

[a] Reagents and conditions: (i) $[BzEt_3N]Cl$ (1 mol %), $[Pd(PPh_3)_4]$ (6 mol %), CuI (10 mol %), aqueous NaOH (10 equiv), benzene, 60 °C, 86% for $bpyT_3bpy$ and 42% for $bpyT_5bpy$.

were obtained by cyclic voltammetry and are collected in Table 1; the results for Ru(bpyDBT′) and $[Ru(bpy)_3]^{2+}$ are also listed. For both ligands, two oxidation processes are found; these occur at +0.96 V (irreversible) and +1.30 V (irreversible) for $bpyT_3bpy$ (Figure S2) and at +0.71 V (quasi-reversible) and +0.94 V (quasi-reversible) for $bpyT_5$-bpy. The reduction steps (irreversible) are found at −1.89 V and −1.94 V, respectively. The lowering in potentials on going from $bpyT_3bpy$ to $bpyT_5bpy$ is likely related to the more extended conjugated backbone for the larger sized ligand. Worth noting is the fact that both oxidation processes in $bpyT_5bpy$ are quasi-reversible due to better stabilization of the oxidized species, the radical cation and dication, respectively, in comparison to $bpyT_3bpy$. In the latter case, a tentative explanation might be that the oxidized species is more reactive toward the solvent.

For the binuclear complexes, the first oxidation is found at +1.08 V and +0.91 V, for Ru($bpyT_3bpy$)Ru (Figure S2) and Ru($bpyT_5bpy$)Ru, respectively, which lie at slightly higher potentials compared to the corresponding ligands (ΔE = 120 mV and ΔE = 200 mV) (Table 1). In both cases, the oxidation process is quasi-reversible and takes place by exchange of a single electron, as indicated by a ΔE_p of 70 mV. For the complexes, this outcome points to a thiophene-centered first oxidation step, suggesting the formation of oligothiophene radical cations, and is consistent with a weak intercomponent interaction in the cases of both Ru($bpyT_3$-bpy)Ru and Ru($bpyT_5bpy$)Ru, whose metal-centered oxidation (two-electron step) occurs at +1.33 V and +1.32 V, respectively, in turn highlighting a weak intermetallic interaction. In the case of Ru($bpyT_3bpy$)Ru, the next oxidation at the thiophene fragment could be beneath the oxidation of the Ru center (integration of this oxidation wave corresponds to about three electrons). For the larger Ru($bpyT_5$-bpy)Ru complex, an additional single-oxidation step is found at +1.02 V, which is likely due to a thiophene-based process (leading to formation of an oligothiophene dication).

Table 1. Electrochemical Properties of bpyT$_n$bpy Ligands and Ru(bpyT$_n$bpy)Ru Complexes[a]

	$E^{\circ\prime}$(ox, soln) (V), ΔE_p[b] (mV)	$E^{\circ\prime}$(red, soln) (V), ΔE_p[c] (mV)
bpyT$_3$bpy	+0.96 (irrev)	−1.95 (irrev)
	+1.30 (irrev)	
Ru(bpyT$_3$bpy)Ru	+1.08 (70)	−1.15 (70)*
	+1.33 (90)*	−1.43 (70)*
		d
bpyT$_5$bpy	+0.71 (60)	−1.89 (irrev)
	+0.94 (60)	
Ru(bpyT$_5$bpy)Ru	+0.91 (80)	−1.15 (60)*
	+1.02 (70)	−1.38 (80)*
	+1.32 (70)**	*d*
Ru(bpyDBT′)[e]	+1.26 (60)	−1.18 (60)
		−1.50 (60)
		−1.76 (80)
[Ru(bpy)$_3$]$^{2+}$ [e]	+1.30 (60)	−1.25 (60)
		−1.52 (70)
		−1.79 (70)

[a] The electrolyte was 0.1 M $TBAPF_6$/anhydrous CH_3CN for the complexes and anhydrous CH_2Cl_2 for the ligands, with a concentration of 1−1.5 mM, at room temperature. All potentials (±10 mV) are reported in volts vs a Pt^0 pseudoreference electrode and using Fc^+/Fc as an internal reference. Under these experimental conditions, the Fc^+/Fc is quoted at 0.39 V (ΔE_p = 80 mV) versus the SCE electrode and all processes are monoelectronic. The * symbol corresponds to a trielectronic process as estimated by the integration of the wave. The ** symbol corresponds to a dielectronic process as estimated by the integration of the wave. For the irreversible processes, the peak potentials E_a and E_c are given. [b] Metal- and thiophene-based oxidation. [c] Successive ligand-localized reductions. For the irreversible wave, the peak potential is quoted. [d] The third reduction process is not observed due to a strong adsorption peak. [e] From ref 14, Ru(bpyDBT′) is [(bpy)$_2$Ru(bpy-E-DBT′)]$^{2+}$; see text.

As for reduction, a quasi-reversible redox wave corresponding to the transfer of two electrons (2 × one electron) is observed at $E_{red1} = -1.15$ V for both complexes; another transfer of two electrons is registered at $E_{red2} = -1.43$ and −1.38 V, for Ru(bpyT$_3$bpy)Ru and Ru(bpyT$_5$bpy)Ru, respectively. These values are at slightly more positive potentials compared to those for the parent complex [Ru(bpy)$_3$]$^{2+}$ ($\Delta E_{red1} = 100$ mV, $\Delta E_{red2} = 90-140$ mV), which is likely an effect of the extended π-system in the Ru(bpyT$_n$bpy)Ru complexes (Table 1). Comparison of the reduction properties of the bpyT$_3$bpy ligand to those of the bpyT$_5$bpy ligand (Table 1) indicates that for Ru(bpyT$_3$bpy)Ru and Ru(bpyT$_5$bpy)Ru reduction expectantly occurs at the coordinated bpy ligands and not at the oligomeric thiophene backbones, which are reduced at substantially more negative potentials (−1.95 V for bpyT$_3$bpy and −1.89 V for bpyT$_5$bpy). Most likely, the first two-electron reduction step ($E_{red1} = -1.15$ V) occurs at the two bpy ligands bearing the ethynylene group, and the subsequent step likely involves one bpy ligand from each of the two equivalent metal centers. In conclusion, according to the electrochemical results and our interpretation, the easiest oxidation occurs at the electron-rich oligothiophene bridge, whereas the easiest reduction takes place at the terminal metal complex fragments.

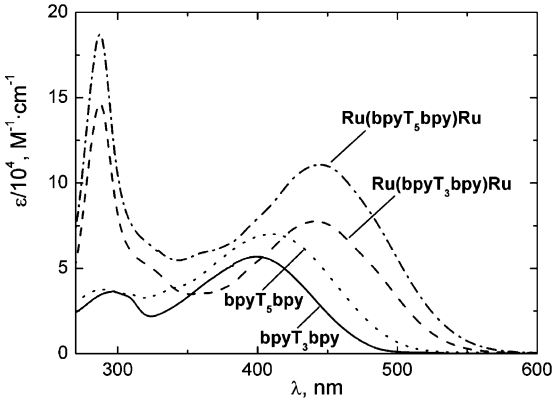

Figure 1. Ground-state absorption spectra. The solvent was CH_2Cl_2 for the ligands and CH_3CN for the complexes.

Steady-State Absorption. Absorption spectra are displayed in Figure 1, and concerned data are collected in Table 2 together with luminescence results to be discussed below; for comparison purposes, results for Ru(bpyDBT′) and [Ru(bpy)$_3$]$^{2+}$ are also displayed. As for the bpyT$_n$bpy ligands, the lowest-energy broad band is mainly due to long-axis $^1\pi,\pi^*$ transitions occurring within the thiophene backbone.[36,64] Some charge transfer (CT) character involving the thiophene units as donors and bpy and ethynylenic fragments as acceptors may also be present.[47] These features are consistent with both the shift from 399 to 410 nm for the peak maximum and the increase in absorption intensity (from ϵ = 56 700 to 70 100 M^{-1} cm^{-1}) on going from bpyT$_3$bpy to bpyT$_5$bpy. This behavior is quite common for thiophene oligomers wherein, on going from smaller to larger modules, electron delocalization is observed to regularly affect the optical absorption properties until a saturation limit is reached (for repeat units $n \geq 5$) in the effective conjugation length.[3,46,47]

Regarding the dimeric complexes, the spectral profiles in Figure 1 reveal the occurrence of intense, narrow, $^1\pi,\pi^*$ bpy-

Table 2. Absorption and Luminescence Properties of bpyT$_n$bpy Ligands and Ru(bpyT$_n$Bpy)Ru Complexes with n = 3, 5[a]

	absorption	emission				
		298 K			77 K	
	λ_{max} (nm), ϵ_{max} (M^{-1} cm^{-1})	λ_{em} (nm)	ϕ_{em}	τ[b] (ns)	λ_{em} (nm)	τ[b] (μs)
bpyT$_3$bpy	296 (36300), 399 (56700)	506	0.096	0.7	527	$<1 \times 10^{-3}$
bpyT$_5$bpy	288 (37600), 410 (70100)	542	0.122	0.6	568	$<1 \times 10^{-3}$
Ru(bpyT$_3$bpy)Ru	288 (146800), 442 (77500)	646	0.4×10^{-3}	180	620[c]	
Ru(bpyT$_5$bpy)Ru	287 (187200), 445 (110700)					
Ru(bpyDBT′)[d]	287 (73500), 453 (11900)	647	0.082	1050	614[e]	
[Ru(bpy)$_3$]$^{2+}$ [f]	288 (76600), 452 (14600)	615	0.015	170	582	5.0

[a] In air-equilibrated solvents, at the indicated temperature, CH_2Cl_2 was used for bpyT$_n$bpy (λ_{exc} = 350 nm for the luminescence spectra and 355 or 370 nm for the lifetimes) and CH_3CN was used for Ru(bpyT$_n$bpy)Ru (λ_{exc} = 400 nm for the luminescence spectra and 465 nm for the lifetimes). [b] Values obtained by monitoring the luminescence peak; single exponential decays were observed in each case. [c] Very weak luminescence intensity. [d] In degassed methanol/ethanol 4/1 (v/v) solutions, from ref 14, RubpyDBT′ is [Ru(bpy)$_2$(bpy-E-DBT′)]$^{2+}$; see text. [e] At 80 K. [f] From refs 22 and 68.

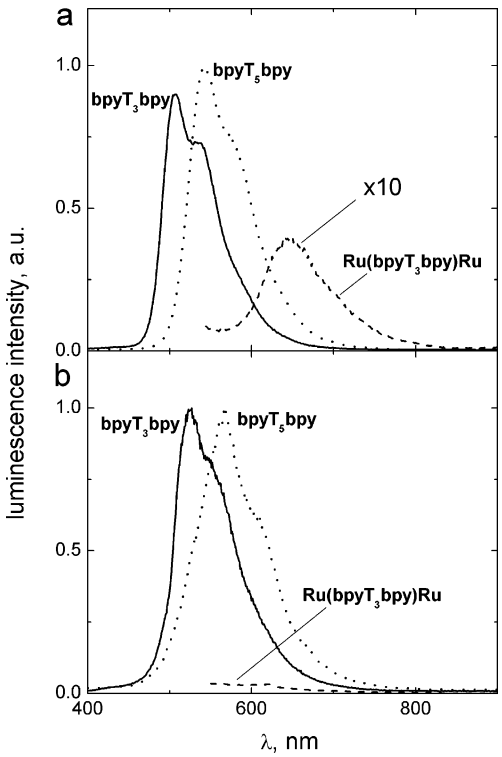

Figure 2. Luminescence spectra at (a) room temperature (scaled according to the luminescence quantum yields, $\lambda_{exc} = 350$ and 400 nm for ligands and complexes, respectively) and (b) 77 K (intensities for $bpyT_3bpy$ and $bpyT_5bpy$ are normalized). The solvent was CH_2Cl_2 for the ligands and CH_3CN for the complexes.

centered transitions, localized in the UV region (287−288 nm, $\epsilon = (1.5-1.9) \times 10^5$ M^{-1} cm^{-1}) and broad band transitions in the visible, that maximize at 442 nm ($\epsilon = 7.8 \times 10^4$ M^{-1} cm^{-1}) and 445 nm ($\epsilon = 11.1 \times 10^4$ M^{-1} cm^{-1}) for Ru($bpyT_3bpy$)Ru and Ru($bpyT_5bpy$)Ru, respectively. For the complexes, the profiles shown in Figure 1 together with literature results for similar Ru−polypyridine−oligothiophene hybrids[14,15] indicate that the bands in the visible are due to overlapping bands from $^1\pi,\pi^*$ transitions at the thiophene backbone and ^{1}MLCT transitions involving the metal centers and the ligands from the coordination environment (possibly with extension to the ethynylenic fragments). The band maxima are quite similar for the two complexes, 442 and 445 nm for Ru($bpyT_3bpy$)Ru and Ru($bpyT_5bpy$)-Ru, respectively, suggesting a predominance of ^{1}MLCT transitions at these wavelengths, with the larger absorption intensity for the latter case being likely due to a larger contribution of the underlying tail from absorption at the thiophene backbone (Table 2 and Figure 1).

Luminescence. Luminescence results are gathered in Table 2 and illustrated in Figure 2, with panel (a) for room temperature and (b) for 77 K spectra; the excitation conditions are indicated in Table 2. For comparison purposes, in this table are also listed results for Ru(bpyDBT′) and [Ru-$(bpy)_3]^{2+}$ complexes.

The $bpyT_3bpy$ and $bpyT_5bpy$ ligands exhibit room temperature (rt) luminescence features (quantum yields $\phi_{em} \sim 0.1$, CH_2Cl_2 solvent) typical for the fluorescence of thiophene-based oligomers;[11,36,42,64] the emission level of the fluorescent state is higher for $bpyT_3bpy$ (peak maximum $\lambda_{em} = 506$ nm, rt) than it is for $bpyT_5bpy$ (peak maximum $\lambda_{em} = 542$ nm, rt), which parallels the behavior found for the lowest-energy absorption bands of the ligands (Figure 1). The luminescence lifetimes of $bpyT_3bpy$ and $bpyT_5bpy$ are 0.7 and 0.6 ns, in agreement with previous reports dealing with similar oligothiophenes.[49]

For the complexes Ru($bpyT_3bpy$)Ru and Ru($bpyT_5bpy$)-Ru, the intense oligothiophene-based fluorescence disappears and is replaced by a very weak luminescence that only for the former was characterized; time-resolved luminescence studies with picosecond resolution indicate that quenching takes place with a rate constant $k > 5 \times 10^{10}$ s^{-1}. For Ru($bpyT_3bpy$)Ru, the observed luminescence features, $\lambda_{em} = 646$ nm, $\phi_{em} = 0.4 \times 10^{-3}$, and $\tau = 180$ ns, at room temperature (see Table 2) are consistent with a metal−ligand charge transfer (^{3}MLCT) nature for the emission.[14,22,24]

The 77 K luminescence results are as follows. For the $bpyT_nbpy$ ligands, the spectral profiles (see Figure 2b) and the lifetime values point to a fluorescence nature of the emission, similar to what happens at room temperature; this is further consistent with the observed red-shift in the emission maximum with respect to the room temperature case (on going from 298 to 77 K, λ_{em} changes from 506 to 527 nm for $bpyT_3bpy$ and from 542 to 568 nm for $bpyT_5$-bpy). This behavior is as expected for $^1\pi,\pi^*$ fluorescent levels.[11,36,42,64] For the complexes, the emission level at 77 K is very weak and, only for Ru($bpyT_3bpy$)Ru, an apparent band maximum at 620 nm was detected (Table 2 and Figure 2). Transient absorption studies (see below) provide evidence for low-lying nonemitting levels in the complexes studied.

Transient Absorption. To get a more detailed description of the nature of the excited states for the examined $bpyT_n$-bpy and Ru($bpyT_nbpy$)Ru compounds, we performed transient absorption (TA) experiments at room temperature with nanosecond TA spectroscopy. Difference transient absorption spectra for the $bpyT_nbpy$ ligands in degassed CH_2Cl_2 as produced by a 355 nm excitation pulse are displayed in Figure 3. The spectra for the ligands are qualitatively similar in the region of the ground-state bleaching, peaking at 400 and 420 nm for $bpyT_3bpy$ and $bpyT_5bpy$, respectively. Likewise, the strong absorption features in the visible region show a similar shape, with peaks at 700 and 760 nm, for $bpyT_3bpy$ and $bpyT_5bpy$, respectively. In the insets of Figure 3, the absorption decays taken at two characteristic wavelengths are also shown, together with curve-fitting results. The kinetics followed a single-exponential law in each case, and the found lifetimes, $\tau_A \sim 19$ and 13.5 μs, respectively, are listed in Table 3. The spectral profiles and the lifetimes agree well with reported triplet−triplet spectra for oligothiophenes of comparable length and are, therefore, assigned to the lowest-lying $^3\pi,\pi^*$ excited states.[48,49,64]

TA spectra for degassed CH_3CN solutions of the Ru-($bpyT_nbpy$)Ru complexes originated by 355 nm excitation are displayed in Figure 4. In the figure, insets show kinetic analyses of the decays, as taken at the indicated wavelength

(64) Becker, R. S.; deMelo, J. S.; Macanita, A. L.; Elisei, F. *J. Phys. Chem.* **1996**, *100*, 18683.

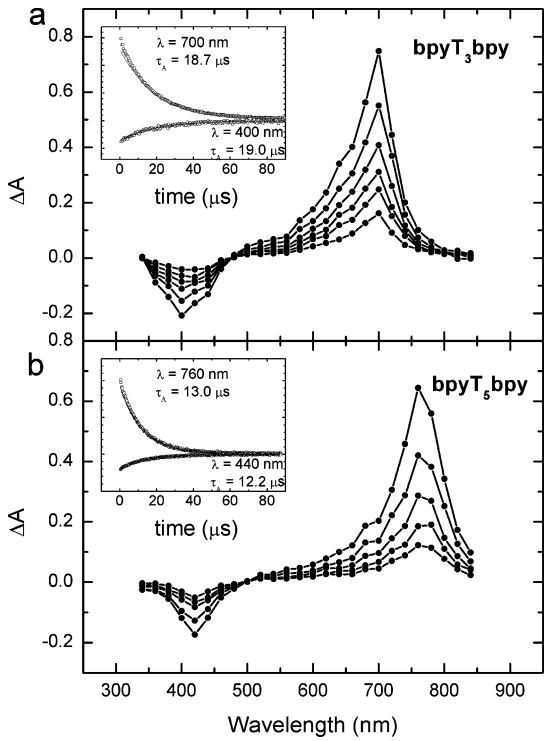

Figure 3. Transient absorption difference spectra for ligands bpyT$_3$bpy (a) and bpyT$_5$bpy (b) in a CH_2Cl_2 degassed solution obtained at various delay times (0−30 μs; see text; inset time decay observed at the indicated wavelength is shown); λ_{exc} was 355 nm, and values for τ_A are also collected in Table 3.

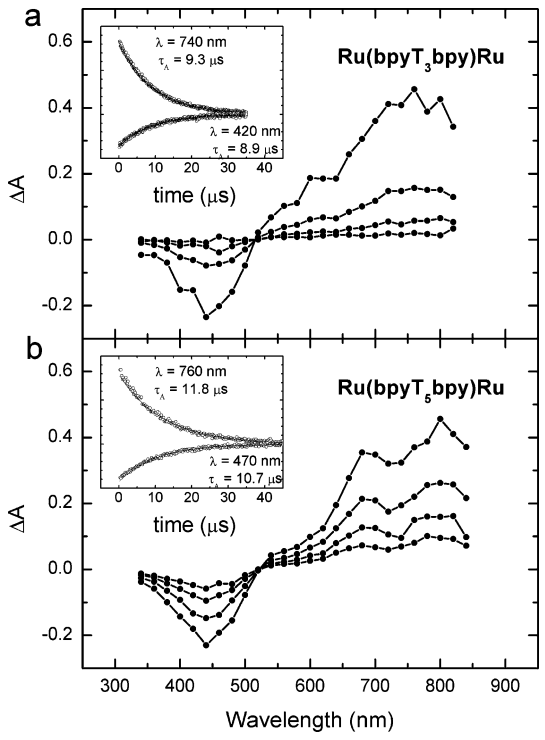

Figure 4. Transient absorption difference spectra for complexes Ru(bpyT$_3$-bpy)Ru (a) and Ru(bpyT$_5$bpy)Ru (b) in a CH_3CN degassed solution obtained at various delay times (0−20 μs; see text; inset time decay observed at the indicated wavelength is shown); λ_{exc} was 355 nm, and values for τ_A are also collected in Table 3.

Table 3. Transient Absorption Results for T$_n$ Ligands and RuT$_n$Ru Complexes with $n = 3, 5$[a]

	λ_{max} (nm)	τ_A[b] (μs) [ns]	state
bpyT$_3$bpy	400	19.0	$^3\pi,\pi^*$
	700	18.7 [270]	
bpyT$_5$bpy	440	12.2	$^3\pi,\pi^*$
	760	13.0 [280]	
Ru(bpyDBT′)[c]		1.2	^{3}MLCT
Ru(bpyT$_3$bpy)Ru	420	8.9	$^3\pi,\pi^* + {}^3$MLCT
	740	9.3 [160]	
Ru(bpyT$_5$bpy)Ru	470	10.7	$^3\pi,\pi^* + {}^3$MLCT
	760	11.8 [135]	

[a] In degassed CH_2Cl_2 (for bpyT$_n$bpy) and CH_3CN (for Ru(bpyT$_n$bpy)Ru) solvents, at room temperature, λ_{exc} = 355 nm; in square brackets are lifetimes obtained in air-equilibrated solutions. [b] Lifetime values obtained by monitoring the indicated wavelength; single exponential decays were observed in each case. [c] From ref 14, Ru(bpyDBT′) is $[Ru(bpy)_2(bpy\text{-}E\text{-}DBT')]^{2+}$; see text.

(see Table 3). For both complexes, the transient absorption spectral profiles feature strong ground-state bleaching, peaking around 440 nm, and an intense, broad absorption band in the visible, near-IR region, with a peak at 760 nm for Ru(bpyT$_3$bpy)Ru and at 800 nm (and a shoulder at 680 nm) for Ru(bpyT$_5$bpy)Ru; the lifetime values are $\tau_A \sim 9$ and 11 μs, respectively. These features are quite different from those shown by a complex studied previously, where a thiophene-ethynyl group was linked to the 5-position of a bpy coordinated ligand, $[(bpy)_2Ru(bpyDBT')]^{2+}$, abbreviated as Ru(bpyDBT′) (Chart 1),[14] and that can be viewed as a useful mononuclear reference unit for our dimeric species. Actually, the transient absorption for Ru(bpyDBT′) exhibited (besides bleaching for the ground-state absorption) an intense, narrow peak around 450 nm and only a rather weak contribution in the range 500−800 nm. Remarkably, for Ru(bpyDBT′), both luminescence and transient absorption properties were ascribed to ^{3}MLCT levels; for instance, τ_{em} and τ_A were 1.05 and 1.2 μs, respectively, in degassed CH_3CN.[14] On the basis of the transient absorption profiles and decays (Table 3), the lowest-lying excited state for both Ru(bpyT$_3$bpy)Ru and Ru(bpyT$_5$bpy)Ru at 298 K appears not to be of a ^{3}MLCT nature.

One may notice that, according to rough estimates based on the electrochemical data of Table 1, CS states with a hole localized on the oligothiophene bridge and an electron localized on the complex (i.e., on the coordinated bpy-ethynyl ligand) could lie at ca. 2.2 eV for Ru(bpyT$_3$bpy)Ru and ca. 2.1 eV for Ru(bpyT$_5$bpy)Ru, i.e., lower in energy by ca. 0.1 eV than the corresponding $^1\pi,\pi^*$ level localized on the oligothiophene fragment, the one that is preferentially populated upon excitation at 355 nm (see Figure 1). Therefore, these CS levels could be implicated in deactivation of the oligothiophene-based $^1\pi,\pi^*$ level (this would not hold true in a rigid solvent at 77 K where destabilization of CS levels is expected, compared to what happens in fluid solutions[65]). TA spectra of oligothiophene cations are known to display absorption bands at lower energies than those for the corresponding $^3\pi,\pi^*$ excited state,[48−51,53,64] which might suggest an identification of the obtained TA spectra as being due to the oligothiophene cation. On the other hand, it seems that in our complexes these CS levels are too high in energy and too far from the lowest-lying states to affect the transient

(65) Chen, P. Y.; Meyer, T. J. *Chem. Rev.* **1998**, *98*, 1439.

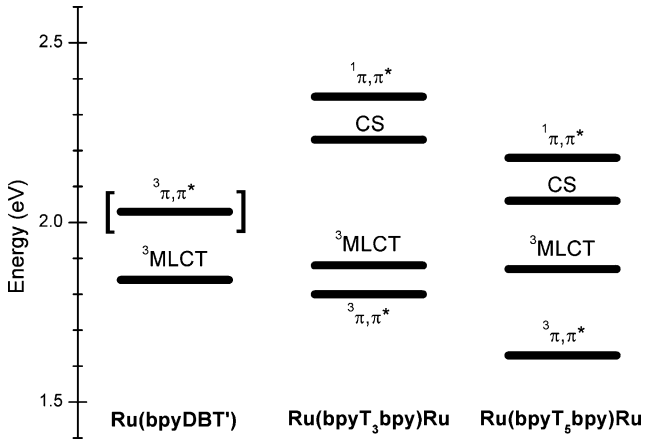

Figure 5. Room temperature energies of the excited states for the compounds studied and for the reference complex Ru(bpyDBT′);[14] at 77 K, the CS levels (of T^+-bpy^- origin) are expected to be strongly destabilized; see text.

absorption features (this will be further discussed below with reference to the energy layout of Figure 5). It can also be mentioned that the registered lifetime values (on the order of 10 μs, Table 3) associated with the TA spectra for our complexes could hardly be compatible with the fact that the oligothiophene-based cation[49−51,53] would be liable to a recombination with a directly connected reduced bpy fragment. In conclusion, for the complexes studied here at room temperature, the lowest-lying levels appear to be predominantly of a $^3\pi,\pi^*$ nature, possibly with some degree of ^{3}MLCT character.

The reactivity with oxygen was tested for all compounds; the lifetime of the lowest-lying $^3\pi,\pi^*$ level of bpyT$_3$bpy and bpyT$_5$bpy in air-equilibrated CH_2Cl_2 solution was 270 and 280 ns, respectively, yielding a rate constant of 1.6×10^9 M^{-1} s^{-1} in both cases. For Ru(bpyT$_n$bpy)Ru, the reactivity with oxygen was higher, and on the basis of the TA lifetimes of 160 ns for Ru(bpyT$_3$bpy)Ru and 135 ns for Ru(bpyT$_5$bpy)Ru in air-equilibrated CH_3CN solutions, a rate constant of 3.5×10^9 M^{-1} s^{-1} was derived. The different reactivities might be ascribable to some difference in the nature of the transients in oligothiophenes and in our binuclear complexes, probably due to some degree of mixing of ^{3}MLCT and $^3\pi,\pi^*$ levels in the latter, as discussed so far.

Energy Levels and Photophysics. Regarding the bpyT$_3$bpy and bpyT$_5$bpy ligands, their fluorescence properties in CH_2Cl_2, related to the lowest-lying $^1\pi,\pi^*$ level, have been discussed above. On the other hand, no phosphorescence was detected for the triplet level, which is a common outcome for thiophene oligomers.[36,42,64,66] Nevertheless, the energy level of the triplet state for several such oligomers has been estimated to lie some 0.55 eV lower than that of the related fluorescent $^1\pi,\pi^*$ singlet.[14,42] For bpyT$_3$bpy and bpyT$_5$bpy, this singlet is located at 2.35 and 2.18 eV, respectively (from the band maximum at 77 K, Table 2), and in turn, the lowest-lying $^3\pi,\pi^*$ triplet is evaluated to lie at ca. 1.80 and 1.63 eV, respectively.

By making use of the available estimates for the energy levels of bpyT$_n$bpy, Ru(bpyDBT′),[14] and Ru(bpyT$_n$bpy)Ru, the diagram of Figure 5 can be drawn. The $^1\pi,\pi^*$ and $^3\pi,\pi^*$ oligothiophene-based levels and the CS levels, of Ru(bpy^--T_n^+-bpy)Ru origin, have been estimated as discussed above. The energy levels for the ^{3}MLCT states have been drawn either from the emission band maximum (when available, i.e., for Ru(bpyT$_3$bpy)Ru and Ru(bpyDBT′)[14]) or from the relation between electrochemical and spectroscopic results involving MLCT states which is known to hold for the complexes of the Ru(II) family, E_{em}^{MLCT} (eV) $\approx$ e(E_{ox} − E_{red}) − 0.6;[22,67] here E_{ox} and E_{red} are the first metal-centered oxidation and ligand-centered reduction, respectively (Table 1). For the complexes, the Ru-based and oligothiophene-based components can be viewed as scarcely interacting (as supported, for instance, by the electrochemical results, Table 1), so that the energy gap between the involved triplet levels can be evaluated by using results for bpyT$_3$bpy and bpyT$_5$bpy. According to this simplified approach, the $^3\pi,\pi^*$−^{3}MLCT energy gap is ΔE_{TT} = 0.08 and 0.22 eV for Ru(bpyT$_3$bpy)Ru and Ru(bpyT$_5$bpy)Ru, respectively. For the former complex, it should be noticed that ΔE_{TT} is small enough to allow some degree of thermal redistribution between ^{3}MLCT and $^3\pi,\pi^*$ levels at room temperature, consistent with the fact that some ^{3}MLCT emission is actually observed in this case, with τ_{em} = 180 ns (Table 2 and Figure 2). On the contrary, for Ru(bpyT$_5$bpy)Ru, no such emission is observed at room temperature; in this case, the TA spectra are expected to be less affected by higher-lying ^{3}MLCT levels and to exhibit a "purer" $^3\pi,\pi^*$ character. At 77 K, thermal redistribution is largely inhibited; in fact, Ru(bpyT$_3$bpy)Ru is very weakly luminescent, and Ru(bpyT$_5$bpy)Ru is not luminescent at all at this temperature.

Conclusions

The dimeric Ru(bpyT$_3$bpy)Ru and Ru(bpyT$_5$bpy)Ru species examined are hybrid systems integrating two types of electroactive and photoactive centers, the $[Ru(bpy)_3]^{2+}$ chromophore and the conjugated oligothiophene wire of variable length. Our investigation affords a description of the possible interplay of excited levels of diverse electronic nature and spatial origin. Light absorption can take place at physically separated subunits and generates accordingly both ^{1}MLCT levels (at the ends of the wire) and $^1\pi,\pi^*$ levels (at the thiophene backbone). The former correspond to metal−ligand charge transfer separation at the terminals of the wire, while the latter levels spread over the oligothiophene backbone because of excitonic delocalization. In principle, charge separated states (CS) can also come into play, corresponding to thiophene-localized oxidation and reduction at a connected bpy ligand from the coordination environment of the Ru(II) center. This rich diversity in the nature of the excited states originated upon light absorption turns into a

(66) Theander, M.; Inganas, O.; Mammo, W.; Olinga, T.; Svensson, M.; Andersson, M. R. *J. Phys. Chem. B* **1999**, *103*, 7771.

(67) Vlcek, A. A.; Dodsworth, E. S.; Pietro, W. J.; Lever, A. B. P. *Inorg. Chem.* **1995**, *34*, 1906.

(68) Balzani, V.; Bardwell, D. A.; Barigelletti, F.; Cleary, F. L.; Guardigli, M.; Jeffery, J. C.; Sovrani, T.; Ward, M. D. *J. Chem. Soc., Dalton Trans.* **1995**, 3601.

simpler picture when examining the layout of the thermally equilibrated levels. Our results indicate that for our species, which contain relatively large oligothiophene backbones, the typical ^{3}MLCT luminescence of $[Ru(bpy)_3]^{2+}$ and its analogues is quenched by the lowest-lying levels, of $^3\pi,\pi^*$ nature, that are delocalized over the oligothiophene backbone. These triplet levels are related to the $^1\pi,\pi^*$ excitonic levels and have the potential to be "conductive" of excitation energy, as confirmed by recent studies wherein Ru- and Os-based ^{3}MLCT levels, located at the terminals of a RuT''_5Os species, are respectively higher in energy and lower in energy (2.1 and 1.6 eV, respectively) than the $^3\pi,\pi^*$ triplet level (1.83 eV, here T''_5 is 2,2′-(3,4,3″,4″,3‴,4‴-hexabutyl-[2,2′:5′,2″:5″,2‴:5‴,2⁗]quinquethien-5,5⁗-diyl)bis-[1,10]-phenanthroline).[54] In conclusion, electrochemical and spectroscopic studies, for this type of binuclear complexes, provide quite useful insights on the interplay of their excited levels, a necessary step in view of the development and exploitation of hybrid materials incorporating oligothiophene-based molecular wires.

Acknowledgment. This research was supported by the CNRS, le Ministère de la Recherche et des Nouvelles Technologies, by the CNR project PM-P03-ISTM-C4/PM-P03-ISOF-M5 (Componenti molecolari e supramolecolari o macromolecolari con proprietà fotoniche ed optoelettroniche), and by the FIRB project RBNE019H9K "Molecular Manipulation for Nanometric Devices" of MIUR.

Supporting Information Available: Figures S1 and S2 including, respectively, NMR and CV data of $bpyT_3bpy$ and $Ru(bpyT_3bpy)Ru$. This material is available free of charge via the Internet at http://pubs.acs.org.

IC050596X